Key Points:
- Coastal vapor transport and California precipitation are modulated by four North Pacific circulation regimes on daily to seasonal timescales
- The most damaging California floods have occurred when these modes were jointly aligned to reinforce onshore flow
- Seasonally, these modes are influenced by ENSO but much variability occurs within the constraints set by the larger-scale climate system

Four Atmospheric Circulation Regimes Over the North Pacific and Their Relationship to California Precipitation on Daily to Seasonal Timescales

Kristen Guirguis[1] ![ID], Alexander Gershunov[1] ![ID], Michael J. DeFlorio[1] ![ID], Tamara Shulgina[1] ![ID], Luca Delle Monache[1] ![ID], Aneesh C. Subramanian[2], Thomas W. Corringham[1] ![ID], and F. Martin Ralph[1] ![ID]

[1]Center for Western Weather and Water Extremes, Scripps Institution of Oceanography, University of California, San Diego, CA, USA, [2]Department of Atmospheric and Oceanic Sciences, University of Colorado, Boulder, CO, USA

Abstract Precipitation in California is highly variable and not well forecasted on subseasonal-to-seasonal (S2S) timescales. Understanding relationships between synoptic-scale atmospheric circulation and hydrometeorological extremes could improve predictability. This work demonstrates the importance of four North Pacific circulation regimes (called the NP4 modes) in modulating precipitation, flooding, and water resources in California. Here we demonstrate how, on daily timescales, interactions between the NP4 modes drive coastal flow that can result in dry conditions from atmospheric ridging or wet conditions associated with enhanced onshore flow and atmospheric river (AR) landfalls. Seasonally, the prevalence of certain NP4 phase relationships can tip the scale toward wet or dry conditions. Relationships between El Niño Southern Oscillation (ENSO) and the NP4 are explored, and we provide insight into the poorly forecasted Western US seasonal precipitation during the "Godzilla" El Niño winter of 2016 by examining climate-weather linkages in a historical context.

Plain Language Summary The amount of precipitation that falls over California in a given water year is highly variable, which presents challenges for water resource management. Skill of both dynamical and statistical models in forecasting precipitation is low at lead times beyond 2 weeks. Recent research has explored relationships between atmospheric circulation patterns and precipitation extremes in the western United States, with the goal of improving predictability. This work demonstrates the importance of four North Pacific circulation regimes in modulating coastal flow patterns that ultimately determines the amount and spatial distribution of precipitation over California on daily and seasonal timescales. We show how the interaction between these modes on daily timescales drives wet and dry episodes within a season. Seasonally, we show how the daily variability occurs within certain constraints established by the larger, more slowly varying climate system, including (but not limited to) El Niño-Southern Oscillation. This work improves understanding of climate-weather relationships, which has implications for predictability of hydrometeorological extremes over California and the western United States.

1. Introduction

California is a densely populated and active agricultural region where demand is high for skillful precipitation forecasts at subseasonal-to-seasonal (S2S) lead times to better optimize water resource management. Most of California's precipitation falls during winter, notably from atmospheric rivers (ARs) that carry large amounts of concentrated moisture to shore (e.g., Gershunov et al., 2017; Zhu & Newell, 1998). Orographic uplift of this moisture-laden air by California's mountain ranges can produce heavy rain, high-elevation snow, and widespread flooding (Ralph et al., 2006, 2011). In Northern California, ARs contribute about half of annual total precipitation (Dettinger et al., 2011), and the presence or absence of a handful of these events can dramatically affect the water supply.

Recently, California was impacted by severe drought from 2012 to 2016, which resulted from a persistent blocking ridge that diverted winter storms away from the coastline. The drought ended abruptly in 2017 following an extremely wet winter associated with unprecedented AR activity (Gershunov et al., 2017; Wang et al., 2017), which caused destructive flooding. The following winters brought more precipitation

variability, with dry conditions in 2018 followed by an extremely wet 2019. This type of variability, which has substantial consequences on life, property, and infrastructure, is typical in California (Dettinger et al., 2011) and is generally not well forecasted at extended-range weather (out to approximately 10 days) or S2S (out to 1 month) lead times (DeFlorio et al., 2018; DeFlorio, Waliser, & Guan, 2019; DeFlorio, Waliser, Ralph, et al., 2019; Nardi et al., 2018; Wick et al., 2013). Projections of future climate suggest that hydroclimate variability in California will intensify as a larger proportion of California's annual precipitation comes in the form of higher-intensity precipitation events separated by longer dry spells, and with more year-to-year variability (Allen & Anderson, 2018; Espinoza et al., 2018; Gershunov et al., 2019; Polade et al., 2014, 2017; Swain et al., 2018; Zecca et al., 2018).

The importance of synoptic-scale atmospheric circulation in modulating AR occurrence, location, and orientation, which affects the amount and spatial distribution of precipitation in the western United States, is well recognized. A growing body of research is aimed at quantifying relationships between large-scale circulation and hydrometeorological extremes to advance predictive capability. Early seminal studies used composite analyses to identify synoptic-scale circulation features linked to AR landfalls along the West Coast (Neiman et al., 2008; Ralph et al., 2004). More recent studies have shown links between known atmospheric teleconnection patterns and AR landfalls (DeFlorio et al., 2018; DeFlorio, Waliser, & Guan, 2019; DeFlorio, Waliser, Ralph, et al., 2019; Guan et al., 2013; Guan & Waliser, 2015; Guirguis et al., 2019; Mundhenk et al., 2016, 2018; Patricola et al., 2020) or dry spells associated with ridging events (Gibson et al., 2020). The teleconnections explored in these studies include the Pacific North American Pattern (PNA), Arctic Oscillation (AO), Madden-Julian Oscillation (MJO), El Niño Southern Oscillation (ENSO), Pacific Meridional Mode (PMM), Quasi-Biennial Oscillation (QBO), and Eastern and Western Pacific Oscillations (EPO, WPO). These regional teleconnections are associated with Rossby wave patterns that affect the strength and position of ridges and troughs over the northern Pacific and western North America.

Previous work described in Guirguis et al. (2018), hereinafter GGR18′, used rotated Empirical Orthogonal Function (REOF) analysis to identify common patterns of winter atmospheric variability and showed that a small subset of these patterns explained most of the variance in AR activity along the West Coast. These were identified as a pressure anomaly in the Gulf of Alaska similar to the EPO, a Canadian-Pacific dipole pattern similar to the PNA, a Baja-Pacific dipole anomaly, and a pressure anomaly off of California's coast. In this work, we refer to these modes jointly as the North Pacific-4 (NP4) modes. Below we demonstrate how the NP4 modes interact to modulate coastal vapor transport and quantify the importance of mode interaction on hydrologic extremes in California on daily and seasonal timescales. We examine the role of the NP4 modes both individually and in combination with each other in driving daily coastal IVT variability, precipitation, and historical flooding in California (sections 3 and 4 below). Seasonally, we show how the NP4 modes tend to prefer one phase over the other in a given water year (WY), which results in recurring flow patterns that help determine a wet or dry winter (section 5). Relationships between ENSO and the NP4 are explored, and we show that on seasonal timescales, ENSO does play an important role, but much variability occurs within the constraints set by ENSO (section 6). We also provide insight into the failed predictions of the rainy season in the western United States despite the strong "Godzilla" El Niño by examining relationships between ENSO and the NP4 modes over the historical record, which has implications for prediction of precipitation over the western U.S. region at S2S lead times.

2. Data and Methods

2.1. Integrated Vapor Transport and AR Detection

To identify historical landfalling ARs, we used the catalog described in Gershunov et al. (2017), which provides information on ARs impacting the West Coast (20° to 60°N) from 1948 to the near present using data from NCEP-NCAR global Reanalysis (Kalnay et al., 1996). The AR detection algorithm identifies a landfalling AR according to established criteria for integrated vapor transport (IVT > 250 kg*m^{-1} s^{-1}), integrated water vapor (IWV > 15 mm), and geometric length (longer than 1,500 km). In this study, as in GGR'18, we identify AR days as those when a coastal grid cell was impacted by an AR for at least two 6-hourly time-steps during a calendar day. The time period of this study is 1 November 1948 to 28 February 2018, where November–February has been shown to be the most active part of the AR season for California (e.g., Gershunov et al., 2017).

2.2. Atmospheric Variables

Daily 500 mb geopotential height (G500) and wind fields are from NCEP-NCAR global Reanalysis (Kalnay et al., 1996). Daily anomalies for each grid cell were obtained by regressing out the annual and semiannual harmonics of the local seasonal cycle using least squares regression analysis.

2.3. Precipitation

Daily precipitation data are from Livneh et al. (2013), which is a gridded product derived from station data interpolated to a 1°/16° latitude–longitude grid. The source data are the cooperative observer (coop) summaries of the day from the National Centers for Environmental Information supplemented by first-order automated surface observing system observations (National Climatic Data Center, 2009). This data set is available for the period 1950–2013.

2.4. Historical California Flood Damages

Information from the National Flood Insurance Program (NFIP) claims and losses, available for the period 1978–2017, are used to identify historical California floods with substantial economic loss. We define the most damaging floods as events with insured losses in excess of $10 million as provided in Corringham et al. (2019). In this study, we focus on floods affecting Northern California.

2.5. El Niño Southern Oscillation

To examine relationships with ENSO, we use the monthly Niño 3.4 index from the Climate Prediction Center, which is derived using sea surface temperatures (SSTs) averaged over 5°S to 5°N and 170° to 120°W in the tropical Pacific Ocean. We define El Niño (La Niña) years as those when the Niño 3.4 index exceeded 0.5 standard deviations above (below) the mean for three consecutive months in the NDJF season.

2.6. North Pacific Teleconnection Patterns

We use four North Pacific teleconnection patterns previously identified in GGR′18 to investigate relationships between mid-tropospheric circulation, coastal vapor transport, and precipitation along California and other parts of western North America on daily to seasonal timescales. These modes were identified using rotated EOF analysis applied to 500 mb geopotential height anomalies over the Pacific Ocean and western United States using established methodology for identifying teleconnection patterns (e.g., Barnston & Livezey, 1987). GGR′18 investigated relationships between 15 modes of atmospheric variability and AR landfall probability along the West Coast and showed that a subset of four modes was most important for AR activity over California, some of which are related to well-known teleconnections such as the PNA and EPO (see Text S1 in the supporting information).

For this new work, we have named these modes according to their geographic centers of action as follows: Baja-Pacific (BP), Alaskan-Pacific (AP), Canadian-Pacific (CP), and Offshore-California (OC), which we refer to collectively as the NP4 modes. We chose to define the NP4 modes such that the positive phase is associated with enhanced onshore flow and elevated AR activity over California. The relationship between these NP4 modes and those identified in GGR′18 is discussed in Text S1. The circulation patterns associated with each of the four modes is shown in Figure 1a, and their influence on IVT and AR landfalls along the coast of western North America is shown in Figure S1. In this study, we use these four modes and their interactions to quantify links between atmospheric circulation with coastal IVT and California precipitation. Further details of the EOF analysis and the NP4 modes are given in Text S1.

2.7. Multiple Regression Analysis

To quantify the influence of the NP4 modes on coastal IVT variance and California precipitation, we use multiple linear regression with interactions (e.g., Wilks, 2006) for both daily and seasonal timescales. For daily timescales, we use the four standardized principal components associated with the NP4 as predictors of daily coastal IVT. The daily model is fit for each day in the record, leaving out the target WY in a cross-validated approach.

For seasonal timescales, we quantify the importance of the NP4 in modulating seasonal precipitation variability over California. Here, we use the seasonal phase prevalence of the NP4 modes as the predictors and seasonal precipitation (NDJF) amount in California at 6×6 km spatial resolution as the predict and. We define seasonal phase prevalence as the number of days in a season that a mode was observed in the
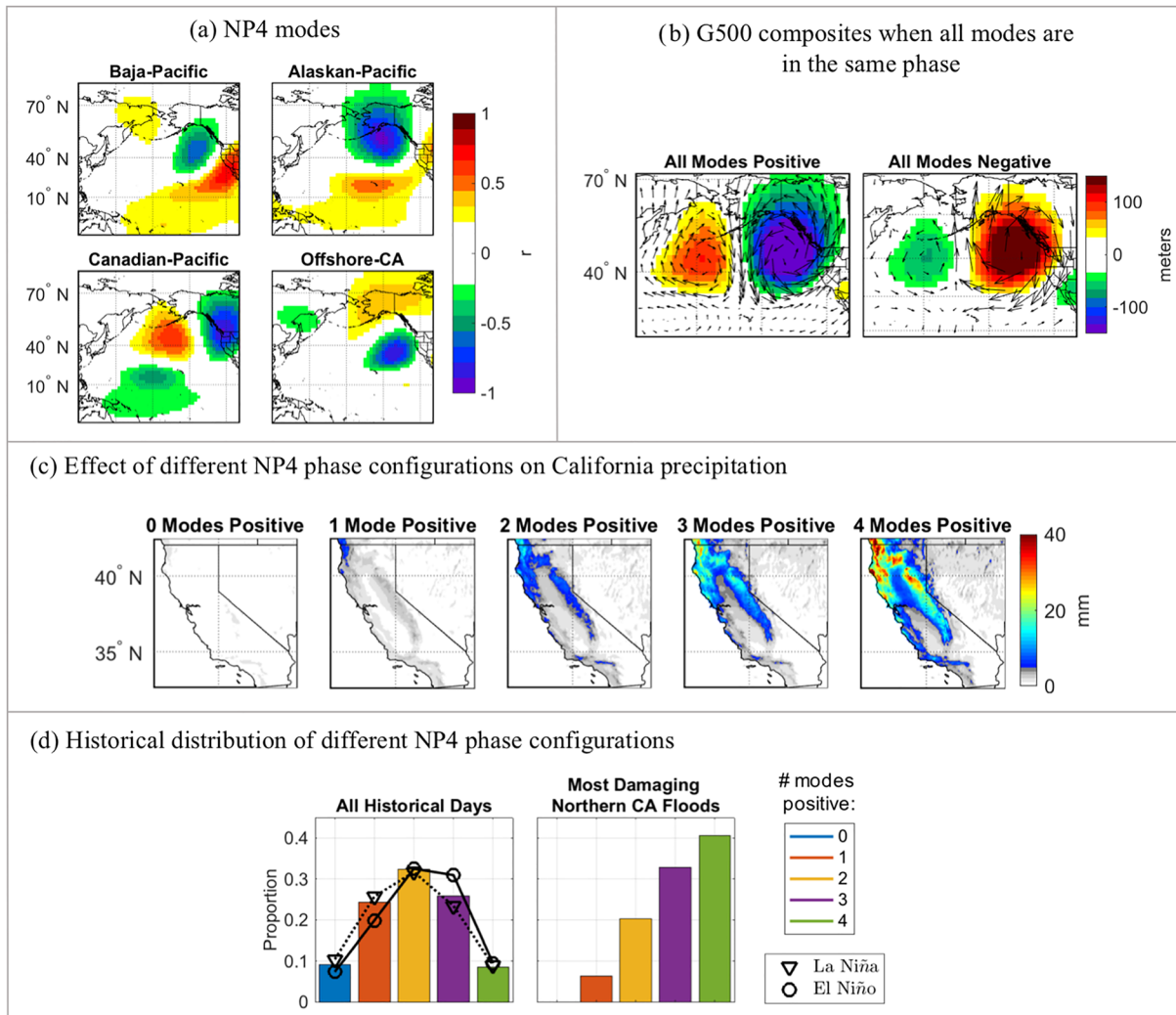
Figure 1. (a) The NP4 modes shown in the phase associated with enhanced AR activity over California. The color scale gives temporal correlation between the associated principal component (PC) and G500 anomalies at a location. (b) Composites of G500 (shaded) and wind speed (vectors) when the NP4 modes are jointly positive (left) or jointly negative (right). (c) Average daily precipitation conditional on the joint phasing of the NP4 modes. (d) Historical probability distribution of different phase configurations for all historical days (left) and the most damaging flood days in Northern California (right). Panel (d, left) also gives the historical probability distribution for La Niña and El Niño years.

positive phase minus the number of days it was in the negative phase. Therefore, this metric provides information on the relative frequency of a ridge versus a trough in a given location. The seasonal model is also cross-validated, leaving out the target WY. Additional details are provided in Text S2.

3. Circulation Regime Interactions and Precipitation Extremes in California

The NP4 patterns shown in Figure 1a collectively explain 60–90% of the local variance in G500 anomalies over a key portion of the northeastern Pacific and along the West Coast (Figure S2). Therefore, they explain much of the large-scale flow that modulates vapor transport over the West Coast. From Figure S1, the positive phase of each mode is associated with anomalous onshore flow and elevated AR activity over California, whereas the negative phase is associated with anomalous offshore flow and reduced California AR activity. On daily timescales, these four modes can interact to become in-phase with each other to reinforce or strengthen a particular flow configuration upstream of the western United States, or they can oppose and counteract each other.

For example, Figure 1b shows the reinforcing effect when four modes are aligned in the positive phase (deep offshore trough, $n = 8\%$ of days) or the negative phase (strong offshore ridge, $n = 9\%$ of days). Other phase

combinations are shown in Figure S4, which gives composites for days when three or more modes are jointly negative (top) or jointly positive (bottom) resulting in distinct flow patterns that generally favor anomalous offshore or onshore flow over California, respectively.

The effect of mode interaction on coastal water vapor transport and AR activity is shown in Figure S5. Joint positive phasing (e.g., three or more modes positive) results in elevated IVT and AR activity over California and the Pacific Northwest whereas joint negative phasing (e.g., three or more modes negative) results in very low IVT and AR activity in these regions. In Northern California at 40°N near the Russian River watershed, the probability of a landfalling AR is 49% when four modes are jointly positive compared with a 2% probability when the modes are jointly negative. Considering all historical ARs affecting the coast at this latitude, 68% of AR days have occurred when three or more modes were jointly positive, compared with 8% that occurred when three or more modes were negative.

This modulation of coastal vapor transport, in turn, affects precipitation in California. From Figure 1c, we observe a strong relationship between the distribution and amount of precipitation and joint phasing of the NP4 modes. On average, 57% of total statewide precipitation during 1950–2013 occurred on days when three or more modes were jointly positive compared to 13% that occurred when three or more modes were jointly negative.

Analysis of flood data for Northern California (Figure 1d) revealed that the largest historical impacts were associated with the type of pattern shown in Figure 1b (left) when all modes were positive. While this configuration accounts for only 8% of all historical days (Figure 1d, left), it accounts for 41% of the most damaging flood days in Northern California with an additional 33% of damaging flood days found to occur when three modes were jointly positive (Figure 1d, right). A better understanding of these modes, their interactions, and links to climate-scale teleconnections could improve hydrometeorological forecasts for California, including for large-scale flood events and associated damages.

4. Daily Weather Variability

Within the season, the BP, AP, CP, and OC modes fluctuate on weather timescales with e-folding times on the order of a week or less (calculated as the average time at which the autocorrelation decays to $1/e$). As an example, mode behavior during the recent dry WY2014 and wet WY2017 is shown in Figure S6. While difficult to visualize, these noisy signals describe the short-term, synoptic-scale atmospheric flow patterns over the northeastern Pacific that modulate coastal moisture transport. On a given day, the modes interact as discussed above to modulate the coastal flow along the coast.

A more organized signal that helps explain the observed dry (WY2014) and unprecedented wet (WY2017) conditions is shown in Figure 2a. These figures show the cumulative mode behavior over the course of the season along with the timing of California landfalling ARs. In general, ARs occurred when multiple modes were jointly positive. During WY2017, 93% of landfalling ARs in Northern California at 40°N occurred when three or more modes were jointly positive and zero occurred when three or more modes were jointly negative. During WY2014, joint negative phasing (≥3 modes negative) occurred on 44% of days in the season, resulting in a persistent blocking pattern associated with the resilient ridge that characterized the ongoing California drought (e.g., Bond et al., 2015; Swain et al., 2014). A break in dry conditions occurred in February 2014 when the circulation regime shifted to the positive phase favoring onshore flow with accompanying AR activity beginning on 7 February.

The goal of this work is to demonstrate how the NP4 modes interact to modulate coastal vapor transport and to quantify the importance of this mode interaction on hydrologic extremes in California. To achieve this goal, we applied multiple regression analysis using the daily BP, AP, CP, and OC modes as predictors for daily coastal IVT at different latitudes. Figure 2b shows the cross-validated results for WY2014 (top) and WY2017 (bottom) for latitude 40°N. Figure S7 shows results for other historic dry years (1977 and 1990, left) and historic wet years (1956 and 1998, right). From these examples, the regression model does well at representing the variability in coastal vapor transport associated with the wet and dry years. It captures the below normal IVT of the historic drought years when AR activity was low, as well as the above normal IVT associated with landfalling ARs in the wet years, and it represents the timing of the ARs very well. The correlation between observed and modeled daily IVT ranges from 0.45 to 0.75 (average = 0.62) for these years.
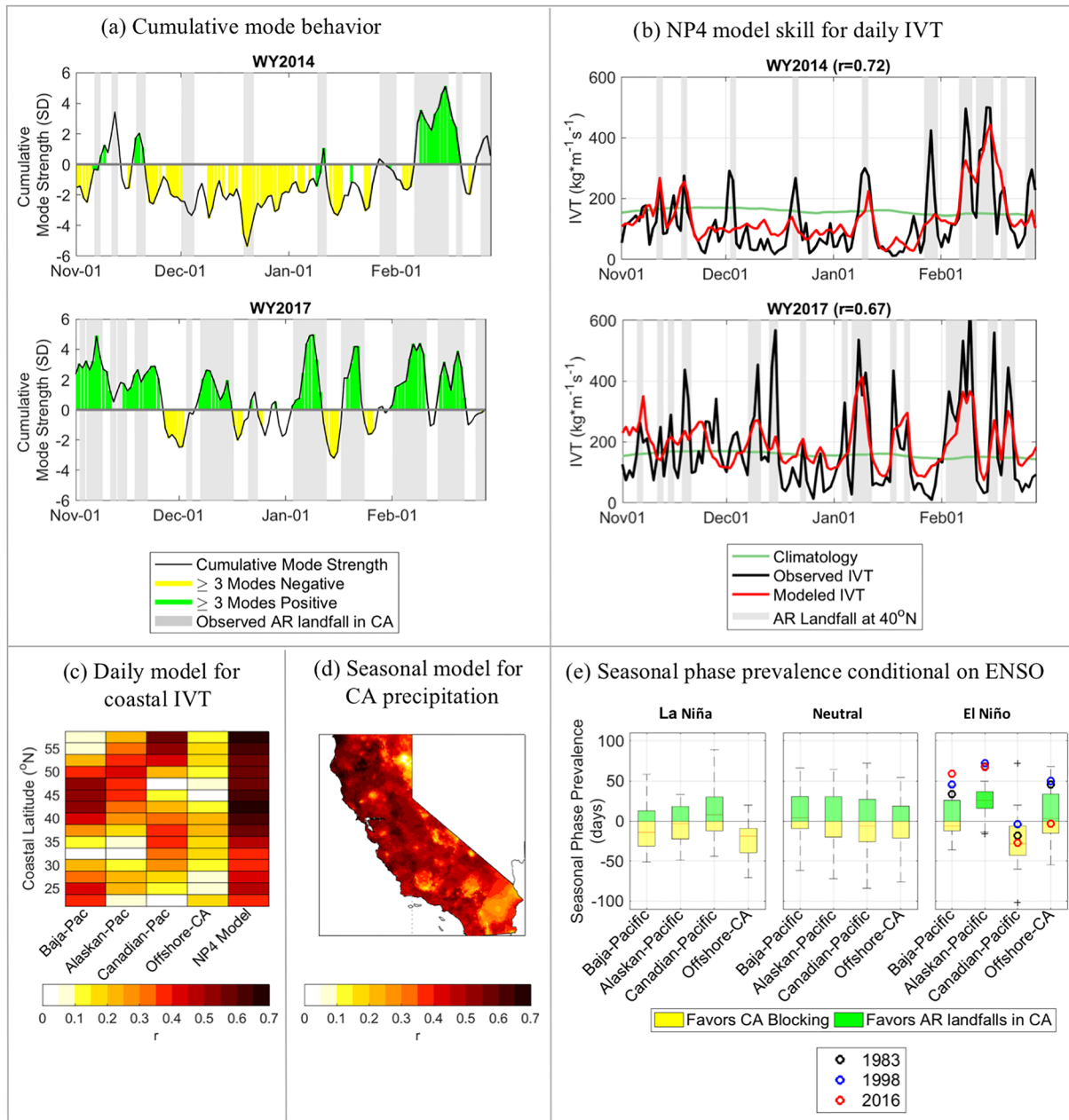
Figure 2. (a) Cumulative mode strength (black line) calculated as the daily sum of the standardized PCs during the dry water year 2014 (top) and wet water year 2017 (bottom). Yellow (green) shading identifies days when ≥3 modes were jointly negative (positive). The timing of ARs impacting California is shown in gray. (b) Cross-validated model results for water years 2014 (top) and 2017 (bottom) for latitude 40°N using the daily NP4 modes as predictors for coastal IVT. Observed daily coastal IVT is shown in black, modeled IVT in red, climatology in green, and timing of landfalling ARs at 40°N in gray. The correlation (r) between modeled and observed IVT is given in the title. (c) Cross-validated results for the entire west coast showing the average correlation (r) between modeled and observed daily coastal IVT for each latitude. Skill using each mode independently is shown in columns 1–4, and skill for the full NP4 model is shown in the fifth column. (d) Cross-validated results of the seasonal NP4 model showing the correlation between modeled and observed seasonal mean precipitation in California. (e) Historical distribution of seasonal phase prevalence conditional on the state of ENSO. A value of +20 on the y-axis means that the mode was present in the positive phase on 20 more days than it was in the negative phase during the season. A value of −20 means the negative phase was more prevalent by 20 days. Strong El Niño years 1983, 1998, and 2016 are emphasized.

Cross-validated results for the entire West Coast are shown in Figure 2c, where in addition to the result of the full NP4 model, we also show the result using each mode independently. The NP4 model is skillful at all latitudes and is superior to any single-mode model. The NP4 model performs best in Northern California, the Pacific Northwest, and Canada. Using climatology as a reference, the daily NP4 model correctly predicts

above (below) normal vapor transport 67% (78%) of the time at 40°N. In Northern California, at this Russian River latitude, this simple statistical model explains 41% of the total daily IVT variance. These results suggest that if we could predict these four modes of synoptic atmospheric variability (which has yet to be studied), then we would do well at predicting subseasonal vapor transport and AR activity. We know that current dynamical forecast models do not provide reliable, accurate forecasts of AR landfalls or precipitation at S2S lead times (e.g., DeFlorio, Waliser, Ralph, et al., 2019). Evaluating the degree to which the NP4 modes are forecasted would be useful for quantifying limits to predictability or identifying forecasts of opportunity for resource management decisions.

5. Seasonal Hydroclimate Variability

Although the NP4 modes fluctuate on short-term weather timescales, an opportunity for seasonal predictability exists. Our findings demonstrate how one or more modes can exist dominantly in one preferred phase over the other during the course of a season, which could be linked to larger scale, more slowly varying components of the climate system. Figure S8 shows the daily distribution of mode phase and strength during the three dry years (1977, 1990, and 2017, top) and three wet years (1956, 1998, and 2017, bottom). The color scale indicates whether a given phase is favorable to blocking (yellow) or enhanced onshore flow (green) over California. In the wet WY2017, enhanced onshore flow and AR activity dominated throughout the season over California due to the positive phase prevalence of multiple modes. During that season, the BP and CP modes were predominantly positive (73% and 66% of the time, respectively) as was the OC mode, though to a lesser extent (59% of the time). By comparison, WY2014 was predisposed toward anomalous offshore flow and blocking because three of the four modes (AP, CP, and OC) were predominantly negative in that season.

During all three historic dry years, a commonality is that multiple modes were predominantly negative, whereas during the wet years the positive phase dominated for multiple modes. It is worth noting that from the mode-preference perspective, all dry years do not look alike, nor do all wet years (Figure S8). For example, in WY1998 (a strong El Niño year), the BP, AP, and OC modes were all decidedly positive, whereas different mode phase preferences are seen in WY1956 (a moderate La Niña year) and WY2017 (a weak La Niña year). Similar differences are seen among the dry years. Therefore, it is not always the same group of modes that tips the season toward wet or dry conditions, suggesting dry and wet periods can be caused by a variety of underlying circulation regimes. These differences point to the possibility of different climate-scale driving mechanisms, which have implications for seasonal predictability. A hypothesis, which is suggested by Figure S8, is that in a given WY, the positive or negative phase of one or more modes might be preferred, possibly due to interannual-to-decadal climate forcing. This seasonal phase prevalence will result in certain reoccurring flow patterns and can result in anomalously wet or dry conditions in a given season.

To quantify the relationship between the NP4 modes and California precipitation on seasonal timescales, we applied multiple linear regression using mode phase prevalence (number of days positive minus number of days negative) as the predictors of seasonal precipitation in California. The cross-validated results are shown in Figure 2d, which gives the temporal correlation between observed and predicted seasonal precipitation for each 6×6 km^2 grid cell. The seasonal prevalence of the NP4 modes explains a substantial amount of the interannual variability in California precipitation. The NP4 collectively account for over 25% of the variance ($r > 0.5$) for much of California (~41% of the domain). For some Northern California locations, the simple NP4 seasonal model explains over 50% ($r > 0.7$) of the interannual precipitation variability. Figure S9 shows the regression results for the grid cell centered over Mendocino County near the Russian River watershed, where the NP4 modes explain about 37% ($r = 0.6$) of the seasonal variance in seasonal precipitation. For this location, the seasonal NP4 model successfully predicts above or below normal precipitation 78% of the time over the 63-year observational record.

6. The Role of ENSO

Having established the importance of interacting North Pacific atmospheric teleconnection patterns on California's hydroclimate on daily and seasonal timescales, we now explore relationships between the seasonal phase prevalence of the NP4 modes and ENSO. Among our research questions is whether this methodology can help to elucidate some differences between the poorly forecasted and drier than expected El Niño winter of 2016 versus the wetter El Niño winters of 1983 and 1998.

Figure 2e shows the historical distribution of the seasonal phase prevalence for each of the NP4 modes conditional on the state of ENSO. In these plots, a value of +20 on the *y*-axis means that the mode was present in the positive phase on 20 more days than it was in the negative phase during the season. A value of −20 means the negative phase was more prevalent by 20 days. We see that El Niño favors the negative phase of the CP mode and the positive phase of the other three modes, whereas the opposite is seen for La Niña (although the AP mode appears less influenced by La Niña than El Niño). This shows that ENSO stacks the deck toward a certain set of weather patterns, which is what statistical seasonal prediction models tap into (Gershunov, 1998). However, within the season, there is still substantial variability, and the resulting weather impacts depend on the timing and extent to which the modes synchronize on daily timescales to reinforce or oppose each other.

From the El Niño plot, we see how the 1983 and 1998 El Niño seasons (which were very wet) and the 2016 El Niño season (which was close to average in terms of California precipitation and not as wet as generally predicted) compared. In all three seasons, the BP and AP modes were strongly positive, as expected from the historical distribution (though these 3 years were at the high end of the distribution). Also in all three seasons, the CP mode was predominantly negative, as expected from the historical distribution (though more so for the 2016 season). A notable difference in mode behavior between these seasons can be seen in the OC mode. In 1983 and 1998, this mode was predominantly positive, whereas it was predominantly negative in 2016. In the positive phase (as was prevalent in 1983 and 1998), the enhanced flow would be directed toward California. In the negative phase (as was prevalent in 2016), the flow would be diverted away from California due to an anomalous offshore ridge, sending AR activity north toward Northern California and the Pacific Northwest, which is what was observed during that year. Interestingly, the prevalence of the negative phase of the OC mode during 2016 was not unusual, but rather fell near the historical median value, whereas the prevalence of the positive phase in 1983 and 1998 was extreme (~92nd and 96th percentile, respectively).

Above in section 3, we showed that the most damaging Northern California floods occurred when the NP4 modes were jointly aligned in the positive phase (c.f. Figure 1d). The question then arises: was this joint phasing influenced by the state of ENSO? From Figure 1d (shown in black), we find that the probability of joint phasing is slightly higher during El Niño than during La Niña. The probability that three modes will align on daily timescales is 23%, 25%, and 31% for La Niña, Neutral, and El Niño, respectively, where the difference between La Niña and El Niño is statistically significant ($\alpha = 0.05$ using resampling). Interestingly, the probability that all four modes will align in the positive phase, which is the pattern most strongly associated with Northern California floods, is unchanged by the state of ENSO, suggesting that the likelihood of damaging floods over Northern California is only modestly dependent on ENSO phase. This is consistent with the findings of Corringham and Cayan (2019) who studied historical flood damages and found a mixed ENSO signal for Northern California, which lies at the fulcrum of ENSO influence. However, it is worth noting that, for Southern California, flood damages were more prevalent during El Niño than La Niña. Identifying the mode phase combinations associated with flooding in Southern versus Northern California would be a worthy topic of future research.

7. Discussion

This study elucidates linkages between daily and seasonal drivers of precipitation extremes in California. In particular, we show the importance of four North Pacific teleconnection patterns (called the NP4 modes) and demonstrate how on daily timescales the alignment of certain phases of the NP4 creates favorable conditions for enhanced onshore flow, AR landfalls, and flooding, while different configurations favor dry conditions associated with upstream atmospheric ridging over the eastern North Pacific basin. Seasonally, there is a tendency for these modes to favor one phase over the other, and this seasonal phase prevalence predisposes weather systems toward certain flow regimes that persist or reoccur during the season, which helps determine if a season is anomalously wet or dry. We investigated relationships between the seasonal phase prevalence of the NP4 modes and ENSO. An important result is that the prevalence of the ridge offshore from California during the winter of 2016, that was blamed for diverting storms away from California (which was identified by one of the NP4 modes), was found to be within the normal range of historical variability, whereas the atmospheric flow conditions during 1983 and 1998 were more anomalous, even for El Niño

years. This could reflect differences in the spatial footprint of SST anomaly patterns observed in these seasons, which has been linked to different precipitation responses, or it could highlight the importance of internal atmospheric variability (Jong et al., 2018; Lee et al., 2018; Kumar & Chen, 2016; Paek et al., 2017, Patricola et al., 2020). An improved understanding of the intraseasonal behavior of the NP4 and linkages to larger scale, more slowly varying components of the climate system, including (but not limited to) ENSO, has the potential to improve seasonal predictions by illuminating important hybrid climate-weather linkages.

These results, therefore, have implications for S2S predictability. Given the importance of the NP4 modes in modulating precipitation in California, an investigation of dynamical model skill in representing these mode interactions on S2S timescales could improve understanding of model predictability and limitations, particularly regarding the extent to which failed forecasts are due to the misrepresentation of large-scale dynamics versus smaller-scale processes, such as those associated with orographic precipitation mechanisms. Currently, dynamical forecasts lack reliable skill at forecasting individual AR events beyond about a week (e.g., DeFlorio et al., 2018; Wick et al., 2013) and aggregate AR activity beyond 2–3 weeks (DeFlorio, Waliser, & Guan, 2019; DeFlorio, Waliser, Ralph, et al., 2019).

This methodology could also be applied to climate model projections. Analysis of the NP4 interactions and associated hydrometeorological impacts could help quantify the degree to which the projected increasingly volatile precipitation regime (e.g., Gershunov et al., 2019; Polade et al., 2014, 2017; Swain et al., 2018) is due to changes in the large-scale circulation in addition to the thermodynamic effects of a warmer atmosphere. With that, the need for reliable forecasts is becoming even more urgent as water resource managers are faced with increasing challenges associated with sourcing the water supply, maintaining hydroelectric power, and managing floods for a growing population.

References

Allen, R. J., & Anderson, R. G. (2018). 21st century California drought risk linked to model fidelity of the El Niño teleconnection. *npj Climate and Atmospheric Science*, *1*, 21. https://doi.org/10.1038/s41612-018-0032-x

Barnston, A. G., & Livezey, R. E. (1987). Classifications, seasonality, and persistence of low-frequency atmospheric circulation patterns. *Monthly Weather Review*, *115*, 1083–1126. https://doi.org/10.1175/1520-0493(1987)115<1083:CSAPOL>2.0.CO;2

Bond, N. A., Corin, M. F., Freeland, H., & Mantua, N. (2015). Causes and impacts of the 2014 warm anomaly in the NE Pacific. *Geophysical Research Letters*, *42*, 3414–3420. https://doi.org/10.1002/2015GL063306

Corringham, T. W., & Cayan, D. R. (2019). The effect of El Niño on flood damages in the Western United States. *Weather, Climate, and Society*, *11*(3), 489–504. https://doi.org/10.1175/WCAS-D-18-0071.1

Corringham, T. W., Ralph, F. M., Gershunov, A., Cayan, D. R., & Talbot, C. A. (2019). Atmospheric rivers drive flood damages in the western United States. *Science Advances*, *5*(12), eaax4631. https://doi.org/10.1126/sciadv.aax4631

DeFlorio, M. J., Waliser, D. E., & Guan, B. (2019). Global evaluation of atmospheric river subseasonal prediction skill. *Climate Dynamics*, *52*(5-6), 3039–3060. https://doi.org/10.1007/s00382-018-4309

DeFlorio, M. J., Waliser, D. E., Guan, B., Lavers, D. A., Ralph, F. M., & Vitart, F. (2018). Global assessment of atmospheric river prediction skill. *Journal of Hydrometeorology*, *19*(2), 409–426. https://doi.org/10.1175/JHM-D-17-0135.1

DeFlorio, M. J., Waliser, D. E., Ralph, F. M., Guan, B., Goodman, A., Gibson, P. B., et al. (2019). Experimental subseasonal-to-seasonal (S2S) forecasting of atmospheric rivers over the western United States. *Journal of Geophysical Research: Atmospheres*, *124*, 11,242–11,265. https://doi.org/10.1029/2019JD031200

Dettinger, M. D., Ralph, F. M., Das, T., Neiman, P. J., & Cayan, D. R. (2011). Atmospheric rivers, floods and the water resources of California. *Water*, *3*, 445–478.

Espinoza, V., Waliser, D. E., Guan, B., Lavers, D. A., & Ralph, F. M. (2018). Global analysis of climate change projection effects on atmospheric rivers. *Geophysical Research Letters*, *45*, 4299–4308. https://doi.org/10.1029/2017GL076968

Gershunov, A. (1998). ENSO influence on intraseasonal extreme rainfall and temperature frequencies in the contiguous US: Implications for long-range predictability. *Journal of Climate*, *11*, 3192–3203.

Gershunov, A., Shulgina, T., Ralph, F. M., Lavers, D., & Rutz, J. J. (2017). Assessing the climate-scale variability of atmospheric rivers affecting the west coast of North America. *Geophysical Research Letters*, *44*, 7900–7908. https://doi.org/10.1002/2017GRL074175

Gershunov, A., Shulgina, T. M., Clemesha, R. E. S., Guirguis, K., Pierce, D. W., Dettinger, M. D., et al. (2019). Precipitation regime change in Western North America: The role of atmospheric rivers. *Scientific Reports*, *9*(1), 9944 (2019). https://doi.org/10.1038/s41598-019-46169-w

Gibson, P. B., Waliser, D. E., Guan, B., DeFlorio, M. J., Ralph, F. M., & Swain, D. L. (2020). Ridging associated with drought in the Western and Southwestern United States: Characteristics, trends, and predictability sources. *Journal of Climate*, *33*(7), 2485–2508. https://doi.org/10.1175/JCLI-D-19-0439.1

Guan, B., Molotch, N. P., Waliser, D. E., Fetzer, E. J., & Neiman, P. J. (2013). The 2010/2011 snow season in California's Sierra Nevada: Role of atmospheric rivers and modes of large-scale variability. *Water Resources Research*, *49*, 6731–6743. https://doi.org/10.1002/wrcr.20537

Guan, B., & Waliser, D. E. (2015). Detection of atmospheric rivers: Evaluation and application of an algorithm for global studies. *Journal of Geophysical Research: Atmospheres*, *120*, 12,514–12,535. https://doi.org/10.1002/2015JD024257

Guirguis, K., Gershunov, A., Clemesha, R. E. S., Shulgina, T., Subramanian, A. C., & Ralph, F. M. (2018). Circulation drivers of atmospheric rivers at the North American West Coast. *Geophysical Research Letters*, *45*, 12–576. https://doi.org/10.1029/2018GL079249

Guirguis, K., Gershunov, A., DeFlorio, M. J., Shulgina, T., Delle Monache, L., Subramanian, A. C., et al. (2020). In Data from: Four atmospheric circulation regimes over the North Pacific and their relationship to California precipitation on daily to seasonal timescales. *UC San Diego Library Digital Collections*, https://doi.org/10.6075/J0154FJJ

Guirguis, K., Gershunov, A., Shulgina, T., Clemesha, R. E. S., & Ralph, F. M. (2019). Atmospheric rivers impacting Northern California and their modulation by a variable climate. *Climate Dynamics*, *52*(11), 6569–6583. https://doi.org/10.1007/s00382-018-4532-5

Jong, B.-T., Ting, M., Seager, R., Henderson, N., & Lee, D. E. (2018). Role of equatorial Pacific SST forecast error in the late winter California precipitation forecast for the 2015/16 El Niño. *Journal of Climate*, *31*(2), 839–852. https://doi.org/10.1175/jcli-d-17-0145.1

Kalnay, E., Kanamitsu, M., Kistler, R., Collins, W., Deaven, D., Gandin, L., et al. (1996). The NCEP/NCAR 40-year reanalysis project. *Bulletin of the American Meteorological Society*, *77*(3), 437–471. https://doi.org/10.1175/1520-0477(1996)077<0437:TNYRP>2.0.CO;2

Kumar, A., & Chen, M. (2016). What is the variability in US west coast winter precipitation during strong El Niño events? *Climate Dynamics*, *49*(7–8), 2789–2802. https://doi.org/10.1007/s00382-016-3485-9

Lee, S.-K., Lopez, H., Chung, E.-S., DiNezio, P., Yeh, S.-W., & Wittenberg, A. T. (2018). On the fragile relationship between El Niño and California rainfall. *Geophysical Research Letters*, *45*, 907–915. https://doi.org/10.1002/2017GL076197

Livneh, B., Rosenberg, E. A., Lin, C., Nijssen, B., Mishra, V., Andreadis, K. M., et al. (2013). A long-term hydrologically based dataset of land surface fluxes and states for the conterminous United States: Update and extensions. *Journal of Climate*, *26*, 9384–9392.

Mundhenk, B. D., Barnes, E. A., Maloney, E. D., & Baggett, C. F. (2018). Skillful empirical subseasonal prediction of landfalling atmospheric river activity using the Madden–Julian oscillation and quasi-biennial oscillation. *npj Climate and Atmospheric Science*, *1*(1), 7. https://doi.org/10.1038/s41612-017-0008-2

Mundhenk, B. D., Barnes, E. A., Maloney, E. D., & Nardi, K. M. (2016). Modulation of atmospheric rivers near Alaska and the US West Coast by northeast Pacific height anomalies. *Journal of Geophysical Research: Atmospheres*, *121*, 12,751–12,765. https://doi.org/10.1002/2016JD025350

Nardi, K. M., Barnes, E. A., & Ralph, F. M. (2018). Assessment of numerical weather prediction model reforecasts of the occurrence, intensity, and location of atmospheric rivers along the West Coast of North America. *Monthly Weather Review*, *146*(10), 3343–3362. https://doi.org/10.1175/mwr-d-18-0060.1

National Climatic Date Center, 2009: Data Documentation for Data Set 3200 (DSI-3200): Surface Land Daily Cooperative Summary of the Day, Report Asheville, NC (www1.ncdc.noaa.gov/pub/data/documentlibrary/tddoc/td3200.pdf)

Neiman, P. J., Ralph, F. M., Wick, G. A., Lundquist, J. D., & Dettinger, M. D. (2008). Meteorological characteristics and overland precipitation impacts of atmospheric rivers affecting the West Coast of North America based on eight years of SSM/I satellite observations. *Journal of Hydrometeorology*, *9*, 22–47.

Paek, H., Yu, J.-Y., & Qian, C. (2017). Why were the 2015/2016 and 1997/1998 extreme El Niños different? *Geophysical Research Letters*, *44*, 1848–1856. https://doi.org/10.1002/2016gl071515

Patricola, C. M., O'Brien, J. P., Risser, M. D., Rhoades, A. M., O'Brien, T. A., Ullrich, P. A., et al. (2020). Maximizing ENSO as a source of western US hydroclimate predictability. *Climate Dynamics*, *54*(1-2), 351–372. https://doi.org/10.1007/s00382-019-05004-8

Polade, S. D., Gershunov, A., Cayan, D. R., Dettinger, M. D., & Pierce, D. W. (2017). Precipitation in a warming world: Assessing projected hydro-climate changes in California and other Mediterranean climate regions. *Scientific Reports*, *7*(1). https://doi.org/10.1038/s41598-017-11285-y

Polade, S. D., Pierce, D. W., Cayan, D. R., Gershunov, A., & Dettinger, M. D. (2014). The key role of dry days in changing regional climate and precipitation regimes. *Natural Science*, *4*, 1–8.

Ralph, F. M., Neiman, P. J., Kiladis, G. N., Weickman, K., & Reynolds, D. W. (2011). A multiscale observational case study of a Pacific atmospheric river exhibiting tropical-extratropical connections and a mesoscale frontal wave. *Monthly Weather Review*, *139*(4), 1169–1189. https://doi.org/10.1175/2010MWR3596.1

Ralph, F. M., Neiman, P. J., & Wick, G. A. (2004). Satellite and CALJET aircraft observations of atmospheric rivers over the eastern North-Pacific Ocean during the El Niño winter of 1997/98. *Monthly Weather Review*, *132*, 1721–1745.

Ralph, F. M., Neiman, P. J., Wick, G. A., Gutman, S. I., Dettinger, M. D., Cayan, D. R., & White, A. B. (2006). Flooding on California's Russian River: Role of atmospheric rivers. *Geophysical Research Letters*, *33*, L13801. https://doi.org/10.1029/2006GL026689

Swain, D. L., Langenbrunner, B., Neelin, J. D., & Hall, A. (2018). Increasing precipitation volatility in twenty-first-century California. *Nature Clim Change*, *8*(5), 427–433. https://doi.org/10.1038/s41558-018-0140-y

Swain, D. L., Tsiang, M., Haugen, M., Singh, D., Charland, A., Rajaratnam, B., & Diffenbaugh, N. S. (2014). The extraordinary California drought of 2013/2014: Character, context, and the role of climate change. *Bulletin of the American Meteorological Society*, *95*, S3–S7.

Wang, S., Yoon, J., Becker, E., et al. (2017). California from drought to deluge. *Nature Climate Change*, *7*(7), 465–468. https://doi.org/10.1038/nclimate3330

Wick, G. A., Neiman, P. J., Ralph, F. M., & Hamill, T. M. (2013). Evaluation of forecasts of the water vapor signature of atmospheric rivers in operational numerical weather prediction models. *Weather and Forecasting*, *28*(6), 1337–1352. https://doi.org/10.1175/WAF-D-13-00025.1

Wilks, D. S. (2006). *Statistical methods in the atmospheric sciences* (p. 648). Cambridge, MA: Academic Press.

Zecca, K., Allen, R. J., & Anderson, R. G. (2018). Importance of the El Niño teleconnection to the 21st century California wintertime extreme precipitation increase. *Geophysical Research Letters*, *45*, 10,648–10,655. https://doi.org/10.1029/2018GL079714

Zhu, Y., & Newell, R. (1998). A proposed algorithm for moisture fluxes from atmospheric rivers. *Monthly Weather Review*, *126*, 725–735.